A brominated M3 based non-fullerene acceptor: synthesis, material and photovoltaic properties

Elena Zuccalà,[1] Suman Mallick,[1] Lea-Marie Habich,[1] Heinz Amenitsch,[2] Thomas Rath,[1,*] and Gregor Trimmel[1,*]

[1] Institute for Chemistry and Technology of Materials, NAWI Graz, Graz University of Technology, Stremayrgasse 9, 8010 Graz, Austria

[2] Institute of Inorganic Chemistry, NAWI Graz, Graz University of Technology, Stremayrgasse 9, 8010 Graz, Austria

* Corresponding authors: thomas.rath@tugraz.at (T. Rath), gregor.trimmel@tugraz.at (G. Trimmel)

Materials

All starting materials were purchased from commercially available sources and used without further purification, unless otherwise stated. The solar cell materials (PM6, PBDB-T, and M3) were purchased from 1-Material. The solvents and solvent additives used for the fabrication of solar cell devices were purchased from Sigma Aldrich and Merck. The di-aldehyde core, compound A, was also purchased from 1-Material and the end groups (B1 and B2) were purchased from Ossila.

Column chromatography was done using a Biotage "Selekt" automated flash chromatography system with purchased pre-filled columns "Sfär" from Biotage (spherical and irregular silica with particle size from 20 – 60 µm).

Synthesis of compound C1
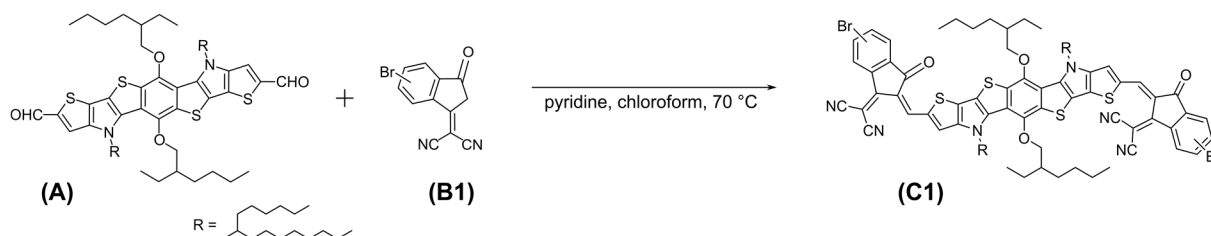
Compound B1, i.e., 2-(5/6-bromo-3-oxo-2,3-dihydro-1H-inden-1-ylidene)-malononitrile (194.0 mg (0.710 mmol) and 102.3 mg (0.0896 mmol) donor dialdehyde core (compound A) were placed in a round bottomed flask, added 25 ml chloroform and purged with nitrogen for 30 minutes. After that, 1 ml pyridine was added and the brownish solution turned dark red. The mixture was stirred over night at 70 °C in an oil bath. TLC (dichloromethane:cyclohexane 1:1) was performed to monitor the reaction progress. Next, 250 ml methanol was added to the solution and left for some hours, leading to a dark red solution with black precipitation, which was filtered with filter paper before the precipitate was

washed with another 30 ml methanol. The raw product was left in the filter paper over night to dry. The raw product was purified via flash column chromatography with Biotage Sfär 100 g pre-packed columns. Fractions were collected in different eprouvettes, the solvent was evaporated under reduced pressure leading to a total amount of 108 mg of compound C1 (yield 73%, dark blue powdered pure product).

^{1}H NMR (300 MHz, CDCl$_3$) δ 8.93 (s, 2H), [8.71 (s), 8.47 (d)] (2H), 7.96-7.75 (m, 6H), 4.77 (d, J = 6.1 Hz, 4H), 4.09 (broad singlet, 4H), 2.12-0.76 (m, 92H) (see **Fig. S7**).

^{13}C NMR (76 MHz, CDCl$_3$) δ 186.95, 186.60, 159.57, 158.95, 148.03, 145.25, 144.84, 141.28, 139.01, 138.40, 138.32, 137.45, 137.05, 135.40, 132.49, 129.87, 129.38, 127.96, 126.78, 126.71, 126.13, 124.60, 120.86, 120.13, 117.18, 114.99, 114.85, 114.57, 79.09, 68.43, 67.95, 52.97, 40.48, 38.99, 31.76, 31.55, 30.63, 30.29, 29.89, 29.40, 29.24, 25.89, 23.58, 23.18, 22.65, 14.18, 11.22 (see **Fig. S8**).

MALDI m/z: [M+H]$^+$ calculated for C$_{792}$H$_{110}$Br$_2$N$_6$O$_4$S$_4$, 1648-1652 (see **Figs. S9, S10**).

Synthesis of compound C2

(A) (B2) (C2)

R =
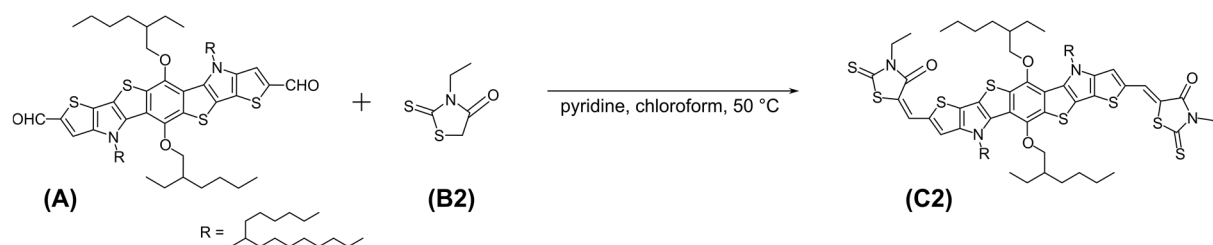
In a round-bottomed flask 128.0 mg (0.7938 mmol) of compound B2, i.e., 3-ethyl-2-thioxothiazolidin-4-one and 103.4 mg (0.0906 mmol) of compound A were dissolved in 25 ml chloroform and purged with nitrogen for 30 minutes. After 30 minutes 1 ml pyridine was added. The mixture did not change its color and was stirred over night at 50 °C in an oil bath. A TLC (dichloromethane:cyclohexane 1:1) showed no complete reaction conversion, so the reaction was left to stir over the weekend for complete conversion of the starting materials. Next, 150 ml methanol was added to the solution and left for some hours. Black precipitation formed and was then filtrated with the filter paper, followed by washing the precipitate with 40 ml methanol. The final purification was done via flash column chromatography using Biotage Sfär 100 g pre-packed columns. Pink fractions were collected in different eprouvettes, the solvent was evaporated under reduced pressure, yielding 110 mg of compound C2 (yield: 85%; pink colored powdered pure product).

^{1}H NMR (300 MHz, CDCl$_3$) δ 7.97 (s, 2H), 7.36 (s, 2H), 4.74 (broad singlet, 4H), 4.20 (d, J = 7.0 Hz, 4H), 4.02 (d, J = 6.6 Hz, 4H), 2.10-0.74 (m, 98H) (see **Fig. S11**).

^{13}C NMR (76 MHz, CDCl$_3$) δ 191.87, 167.36, 146.90, 143.87, 140.58, 136.40, 135.46, 126.97, 123.28, 119.57, 118.52, 117.88, 115.78, 78.49, 52.71, 40.58, 39.92, 38.91, 31.78, 31.62, 30.85, 30.27, 29.85, 29.41, 29.28, 25.94, 23.66, 23.15, 22.80, 22.39, 14.15, 12.32, 11.26 (see **Fig. S12**).

MALDI m/z: [M+H]$^+$ calculated for C$_{78}$H$_{114}$N$_4$O$_4$S$_8$, 1427.6604; found, 1427.6605 (see **Fig. S13**).

Materials characterization methods

NMR spectra were recorded using a Bruker Avance III 300 MHz. All the deuterated solvents were purchased from EurisoTop GmbH. The spectra were referenced to TMS (default) or the solvent signal. The resonance multiplicity is described as s (singlet), d (doublet), t (triplet), and m (multiplet).

Mass spectra were measured using a Micromass TofSpec 2E time-of-flight mass spectrometer from Waters and the appropriate software MassLynx Software V3.5 from Micromass/Waters. Matrices were dithranol or DCTB (trans-2-[3-(4-tertbutylphenyl)-2methyl2-propenylidene]-malononitrile). All spectra were calibrated with polyethylene glycol as external standard.

Absorption spectra of the acceptor materials in **solution** (baseline: chloroform) and **thin film** (baseline: plain glass) were acquired with a Shimadzu UV spectrophotometer UV-1800 used in absorbance mode between 400 nm and 1000 nm.

Cyclic voltammetry (CV) was measured with a BioLogic SP 50 single channel potentiostat, which was coupled with an EC Lab (V11.31) software. The experimental setup was installed in a nitrogen filled glovebox and consisted of three electrodes: a Pt-disk working electrode (d = 2 mm), a Pt-wire counter electrode (d = 0.5 mm) and a non-aqueous $Ag/AgNO_3$ reference electrode (0.5 mm Ag wire in a 0.1 M $AgNO_3$ solution in acetonitrile). The electrolyte solution was prepared with 0.1 M tetrabutylammoniumhexafluorophosphate ($TBAPF_6$) in acetonitrile. Before every new acquisition of CV data, a fresh thin film was drop casted onto the working electrode. The measurements were conducted starting from zero towards positive voltages, with a scan rate of 50 mV/s. A Fc/Fc^+ redox couple was used as reference for setup calibration.

The frontier molecular energies HOMO and LUMO were obtained from the following equations.

$$E_{HOMO} = -(E_{onset\ vs.\ F_c/F_c^+}^{ox} + const.)$$
(1)

$$E_{LUMO} = -(E_{onset\ vs.\ F_c/F_c^+}^{red} + const.)$$
(2)

For this calculation, the value 5.39 eV was applied for the Fermi energy level of NHE vs. vacuum.[1]

In case the reduction peak was not well detectable in the CV scan, the LUMO energy was calculated by subtracting the optical bandgap E_{gap} from the HOMO energy:

$$E_{LUMO} = -(|E_{HOMO}| - E_{gap}).$$
(3)

Grazing-incidence wide-angle X-ray scattering (GIWAXS) measurements were collected at the Austrian 5.2L SAXS Beamline of the ELETTRA Sincrotrone Trieste in Basovizza (Italy). The samples were prepared via drop coating of the active materials on pre-cleaned silicon substrates. The GIWAXS images were acquired at a photon energy of 8 keV with a Dectris Pilatus3 1M detector positioned at a distance of 294 mm from the sample after angular calibration of the detector with silver behenate powder (d-spacing: 58.38 Å). The grazing angle has been set to 1.1° for all the measurements. A blank silicon wafer was additionally measured as background and its scattering profile was then subtracted from the GIWAXS images. For data evaluation, the software packages FIT2D and IGOR Pro 7 (Wavemetrics) were used.

Solar cell characterization methods

Current-voltage (J-V) analysis of the solar cells was performed in inert atmosphere. The setup consisted of a Dedolight DLH400D metal halide lamp with spectrum similar to the AM1.5 sun spectrum as light source, a Keithley Model 2400 Source Measure Unit Instrument and a LabView software for setting and monitoring the measurements. The solar cells were usually characterized between -0.5 V and 1.5 V in sweep mode under a light intensity of 100 mW/cm^2.

Light intensity dependent J-V measurements were carried out with the same setup used for J-V characterization, with the addition of a software-controlled filter wheel containing 9 filters with transmittances from 0.01% to 100%, which was placed between the light source and the measuring box for the solar cells. From the dependence of the V_{oc} on the incident light intensity P_{in}, given by the expression

$$V_{oc} \propto n\frac{k_B T}{q}\ln(P_{in})$$ (4)

where k_B is the Boltzmann's constant, T is the temperature and q is the elementary charge, it was possible to derive the ideality factor n from the linear regression of the slope of the V_{oc} vs. $\ln(P_{in})$ plot.

Similarly, from the relation between J_{sc} and P_{in},

$$J_{sc} \propto P_{in}^{\alpha},$$ (5)

the alpha factor could be obtained by fitting the slope of the J_{sc} vs. P_{in} plot in log-log scale.

The **exciton dissociation probability n_{diss}** and **charge collection efficiency n_{coll}** were extrapolated from the J_{ph} vs. V_{eff} curve plotted in double logarithmic scale. The photogenerated current density J_{ph} is calculated by subtracting the photocurrent density measured under dark conditions (J_D) from the photocurrent density measured under illumination (J_L) ($J_{ph} = J_L - J_D$). The effective voltage V_{eff} is given by $V_{eff} = V_{applied} - V_{oc}$, where $V_{applied}$ is the applied voltage and V_{oc} is the open-circuit voltage.

n_{diss} is then obtained through the ratio between the short-circuit current density J_{sc} and the saturation current density J_{sat} ($n_{diss} = J_{sc} / J_{sat}$), while n_{coll} results from the ratio between the current density at maximum power point J_{mpp} and J_{sat} ($n_{coll} = J_{mpp} / J_{sat}$).

For **external quantum efficiency (EQE) measurements**, a 75 W xenon lamp (Amko Universal Lamp Power Supply LPS210-U) was employed as light source and connected to an Amko MuLTImode4-AT grating monochromator. For all measurements, the incident monochromatic beam was chopped at a frequency of 30 Hz, then the incoming signal was detected with the help of a Keithley Model 2400 source meter and the resulting data were displayed in a LabView program. The system was calibrated with a silicon photodiode (Newport Corporation 818-UV, S/N 11059), then the EQE spectra were recorded within a wavelength range from 380 nm to 1000 nm with a step width of 10 nm.

Thin film thicknesses were determined with a Bruker DektakXT stylus profilometer coupled with the Bruker's Vision64 software for data analysis. The scans were performed over a length of 2000 μm at a speed of 200 μm/s with a stylus of 12.5 μm radius and 3 mg stylus force for a scan resolution of 0.666 μm/pt.

Electron and **hole mobilities** were calculated using the space-charge-limited current (SCLC) method. For this, electron-only and hole-only devices were fabricated with a ITO/ZnO/D:A blend/PNDIT-F3N-

Br/Ag and ITO/PEDOT:PSS/D:A blend/MoO_3/Ag structure, respectively, and characterized with J-V analysis under dark conditions. Electron-only devices were light soaked during 30 minutes before they were measured in the dark, in order to obtain J-V curves without a S-shaped profile.

The mobility values were obtained by linearly fitting the slope *k* of the $J^{1/2}$ vs. V plots between 1 V and 2 V and substituting the extrapolated values for k into the equation

$$k^2 = \frac{9}{8} \frac{\varepsilon_0 \varepsilon_r}{L^3} \mu \tag{6}$$

where μ is the mobility, $\varepsilon_0 \varepsilon_r$ is the permittivity and L is the absorber layer thickness, according to the Mott-Gurney law[2]

$$J = k^2 * V^2. \tag{7}$$

Atomic force microscopy (AFM) images were acquired in tapping mode with a Tosca 400 atomic force microscope by Anton Paar. The cantilevers, also by Anton Paar (AP-ARROW-NCR-10), had a resonance frequency of 285 kHz and a force constant of 42 N/m.
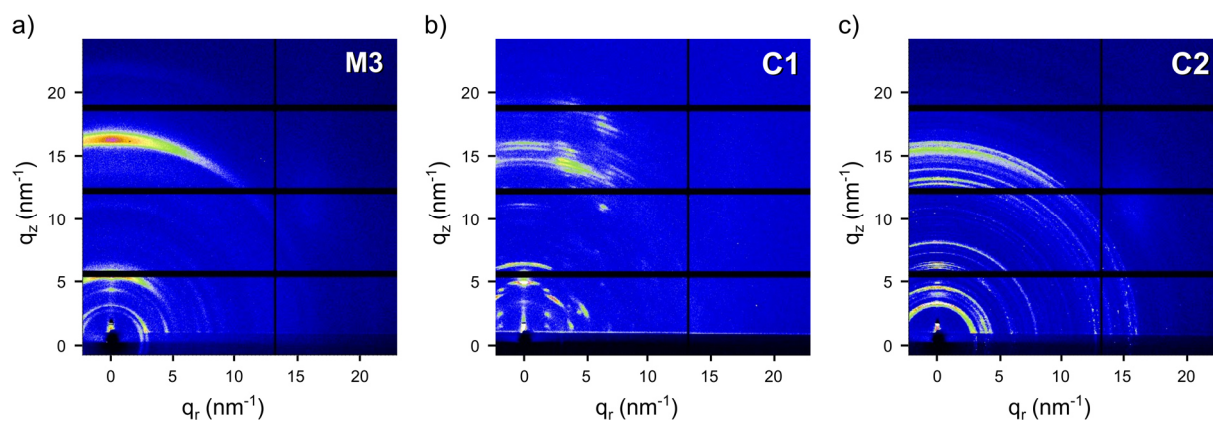
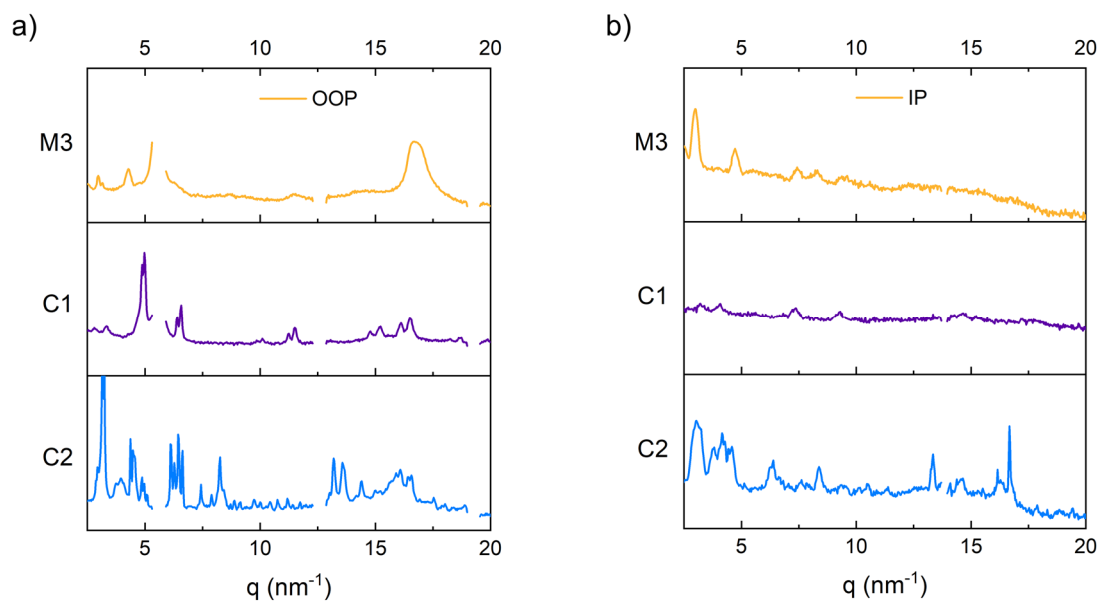**Fig. S1** 2D GIWAXS images of the acceptors a) M3, b) C1 and c) C2.

Fig. S2 Line-cuts in a) out-of-plane and b) in-plane orientation extracted from the 2D GIWAXS images of the acceptors M3, C1 and C2.
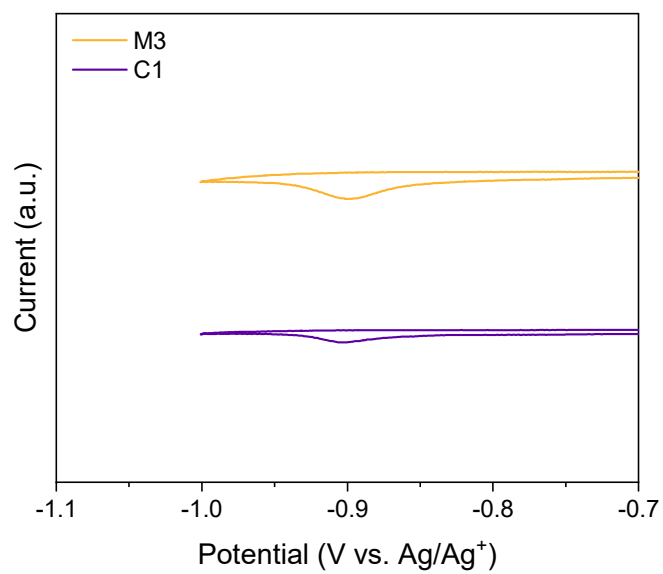
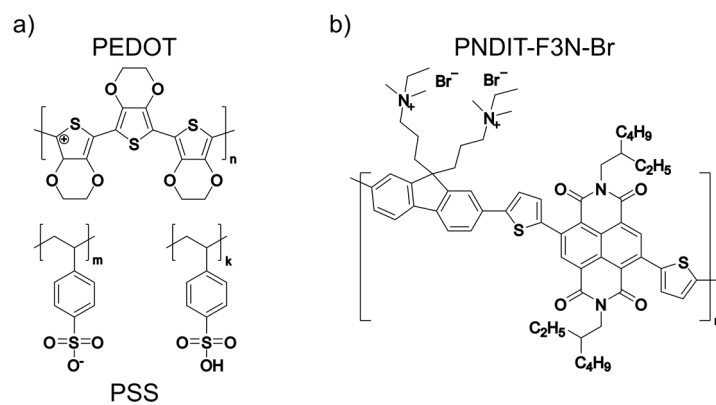**Fig. S3** Reduction peaks of the M3 and C1 acceptors (magnified view).

Fig. S4 Structures of a) the hole transport layer PEDOT:PSS and b) the electron transport layer PNDIT-F3N-Br.

Table S1 Optimization parameters for the PM6:M3 active layer blend processed with different total concentrations (average over 10 devices)

Concentration	V_{oc}	J_{sc}	FF	PCE	Active layer thickness
(mg/ml)	(V)	(mA/cm²)	(%)	(%)	(nm)
12	0.894 (0.884 ± 0.011)	21.1 (20.4 ± 0.7)	68.8 (67.8 ± 2.0)	12.9 (12.2 ± 0.6)	95-100
13	0.894 (0.888 ± 0.010)	22.4 (21.5 ± 0.5)	71.9 (71.4 ± 2.0)	14.4 (13.6 ± 0.4)	100-105
15	0.894 (0.876 ± 0.006)	21.5 (21.6 ± 0.4)	69.6 (68.5 ± 0.8)	13.3 (12.9 ± 0.3)	110-115
16	0.874 (0.856 ± 0.011)	21.1 (20.4 ± 0.4)	59.4 (58.6 ± 1.1)	10.9 (10.2 ± 0.3)	115-120
18	0.854 (0.837 ± 0.009)	20.6 (19.9 ± 0.5)	57.4 (56.2 ± 1.6)	10.0 (9.3 ± 0.3)	125-130

Table S2 Optimization parameters for the PM6:M3 active layer blend (13 mg/ml in 99.5% CF and 0.5% 1-chloronaphthalene; average thickness: ~100 nm) processed with different donor:acceptor ratios and annealing temperatures (annealing time: 5 min; average over 10 devices)

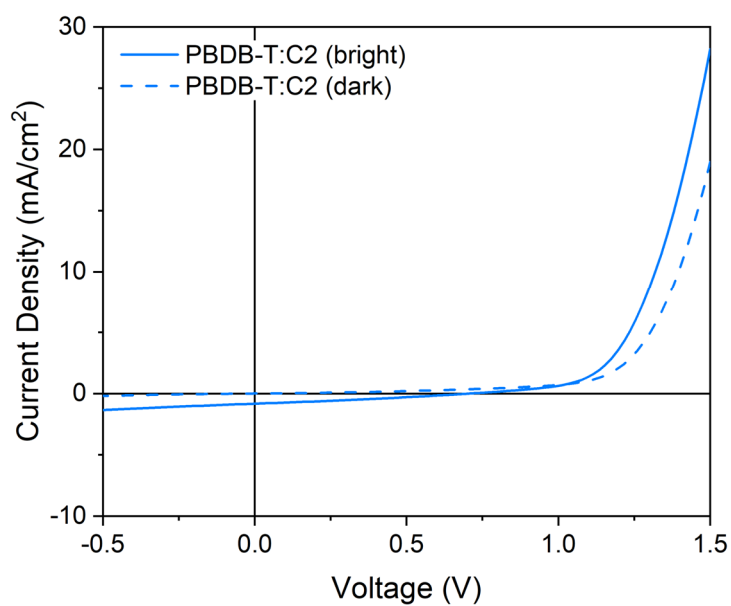| D:A ratio	Annealing T (°C)	V_{oc} (V)	J_{sc} (mA/cm²)	FF (%)	PCE (%)
1:1	90	0.894 (0.888 ± 0.010)	22.2 (21.1 ± 0.6)	70.9 (72.0 ± 1.4)	13.9 (13.4 ± 0.3)
	100	0.874 (0.873 ± 0.001)	21.7 (20.9 ± 0.6)	72.1 (71.9 ± 1.0)	13.7 (13.1 ± 0.4)
1:1.2	90	0.894 (0.886 ± 0.010)	20.2 (19.3 ± 0.6)	72.6 (68.9 ± 4.0)	13.0 (11.8 ± 1.0)
	100	0.874 (0.833 ± 0.054)	-18.9 (19.3 ± 0.9)	73.0 (63.8 ± 7.2)	12.0 (10.3 ± 1.7)

Fig. S5 J-V curve of the best solar cell based on the photoactive blend PBDB-T:C2.

Table S3 J-V characteristic parameters of solar cell devices based on the PBDB-T:C2 active layer blend (average over 15 devices)

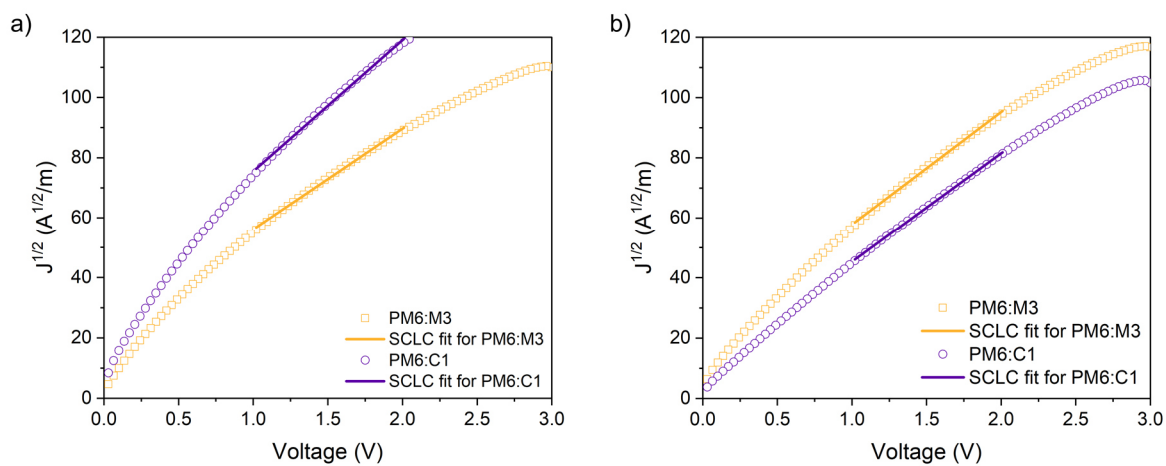|	V_{oc}	J_{sc}	FF	PCE	Active layer thickness
	(V)	(mA/cm^2)	(%)	(%)	(nm)
PBDB-T:C2	0.712 (0.627 ± 0.055)	0.83 (0.73 ± 0.06)	29.0 (28.6 ± 0.5)	0.17 (0.13 ± 0.02)	80

Fig. S6 $J^{0.5}$ vs. V plots of typical a) electron-only and b) hole-only devices and linear fits of the curve slopes performed between 1 V and 2 V used for the calculation of electron- and hole-mobilities of the PM6:M3 and PM6:C1 photoactive blends.
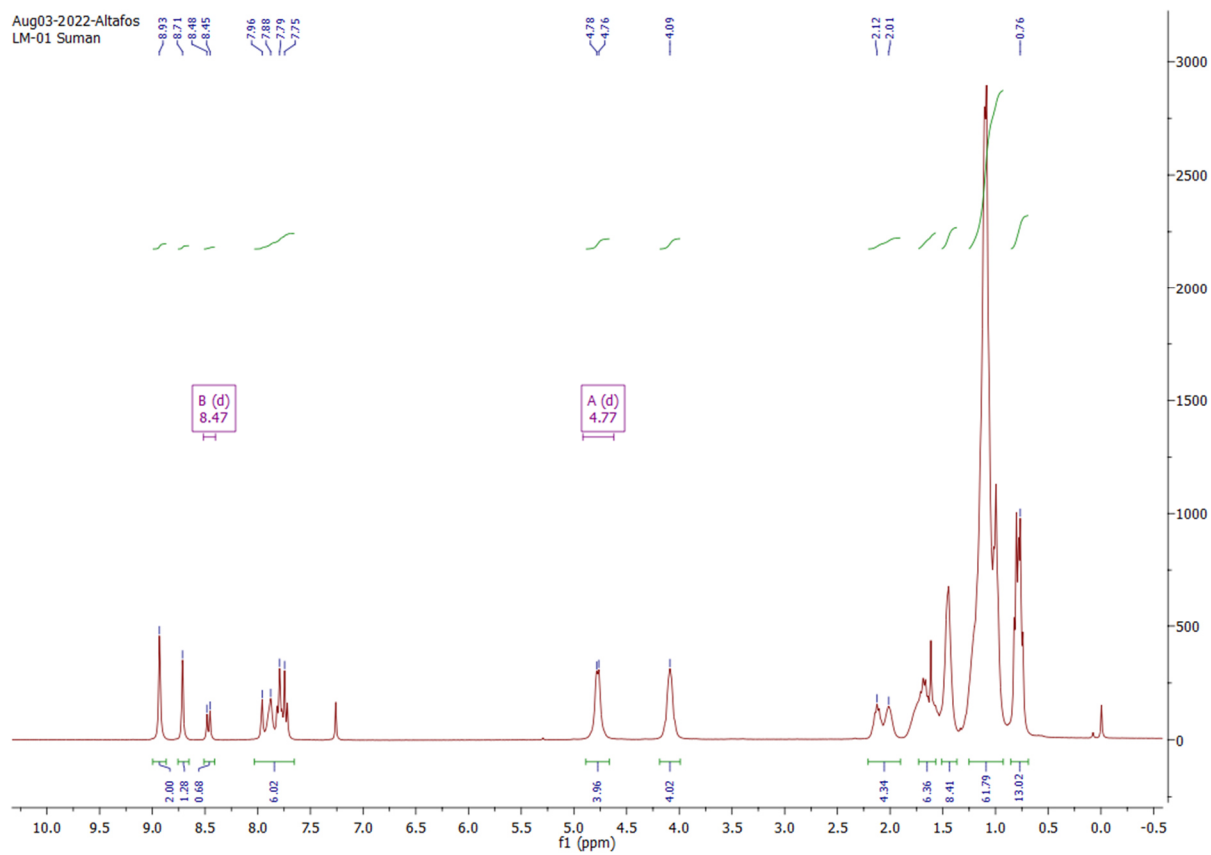
NMR spectra

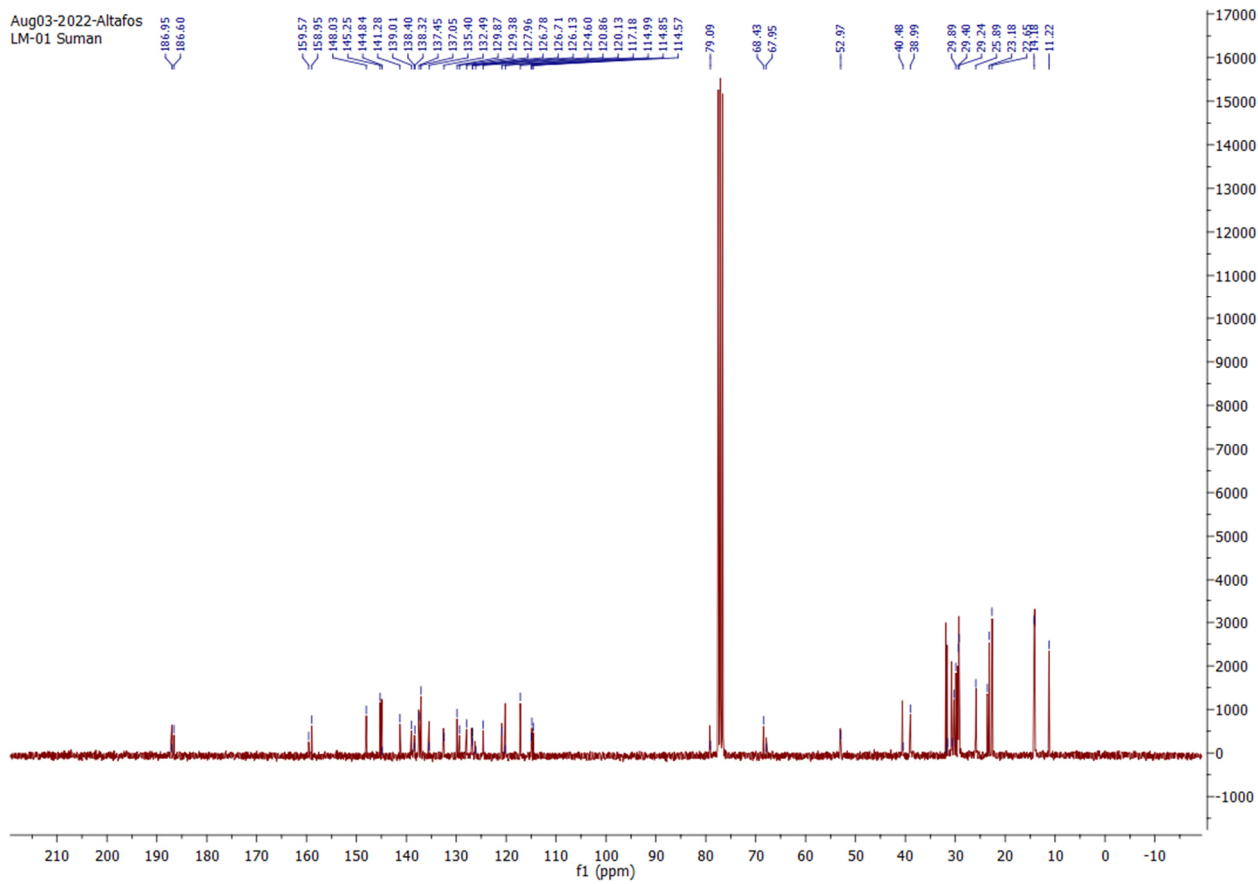**Fig. S7** ^{1}H NMR spectrum of C1 (CDCl₃ solution, ppm, 300 MHz).

Fig. S8 ^{13}C NMR spectrum of C1 (CDCl$_3$ solution, ppm, 76 MHz).

M1-Br_Dithranol (0.015) Is (0.05,1.00) C92H110Br2N6O4S4

TOF LD+
1.97e12

100

%

0

1650.5835
1652.5837
1653.5846
1649.5869 1654.5847
1648.5839
1655.5850
1656.5852

M1-Br_Dithranol 54 (0.899) Sb (99,10.00); Sm (SG, 1x3.00); Cm (2:116)

TOF LD+
824

100

%

0

1652.5607
1651.5847
1653.5632
1650.5826
1654.5662
1649.5811
1655.5692
1648.6061
1656.5726

1426.3424
1425.3380 1428.3522
1451.0488
1085.7321 1144.8324 1201.2513 1301.9722 1378.0011 1539.4519 1592.9128 1657.5764 1736.5947 1835.0695 1867.4335 1887.3999 1974.0931

m/z

1050 1100 1150 1200 1250 1300 1350 1400 1450 1500 1550 1600 1650 1700 1750 1800 1850 1900 1950
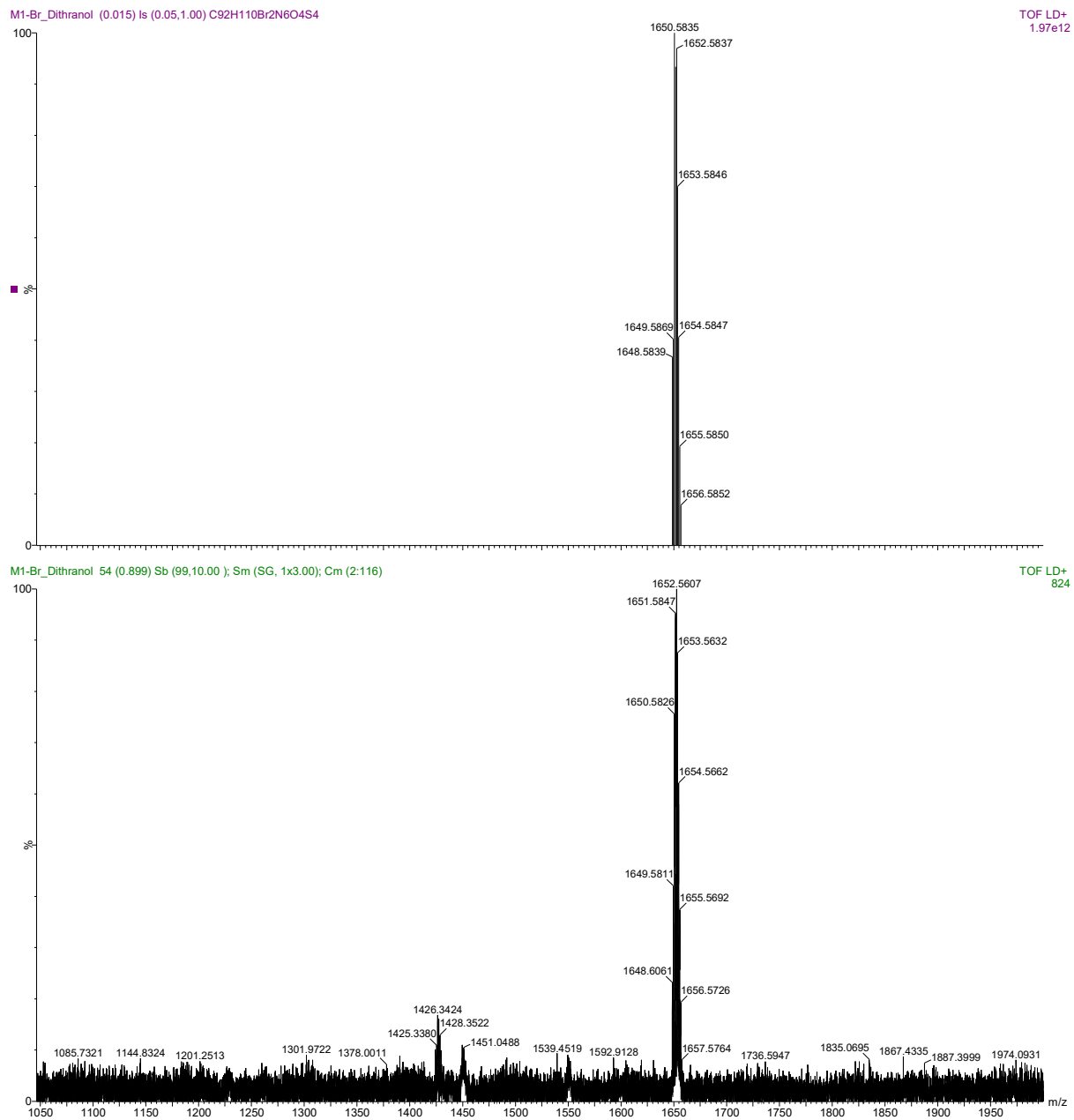
Fig. S9 MALDI-TOF mass spectrometry data of C1.
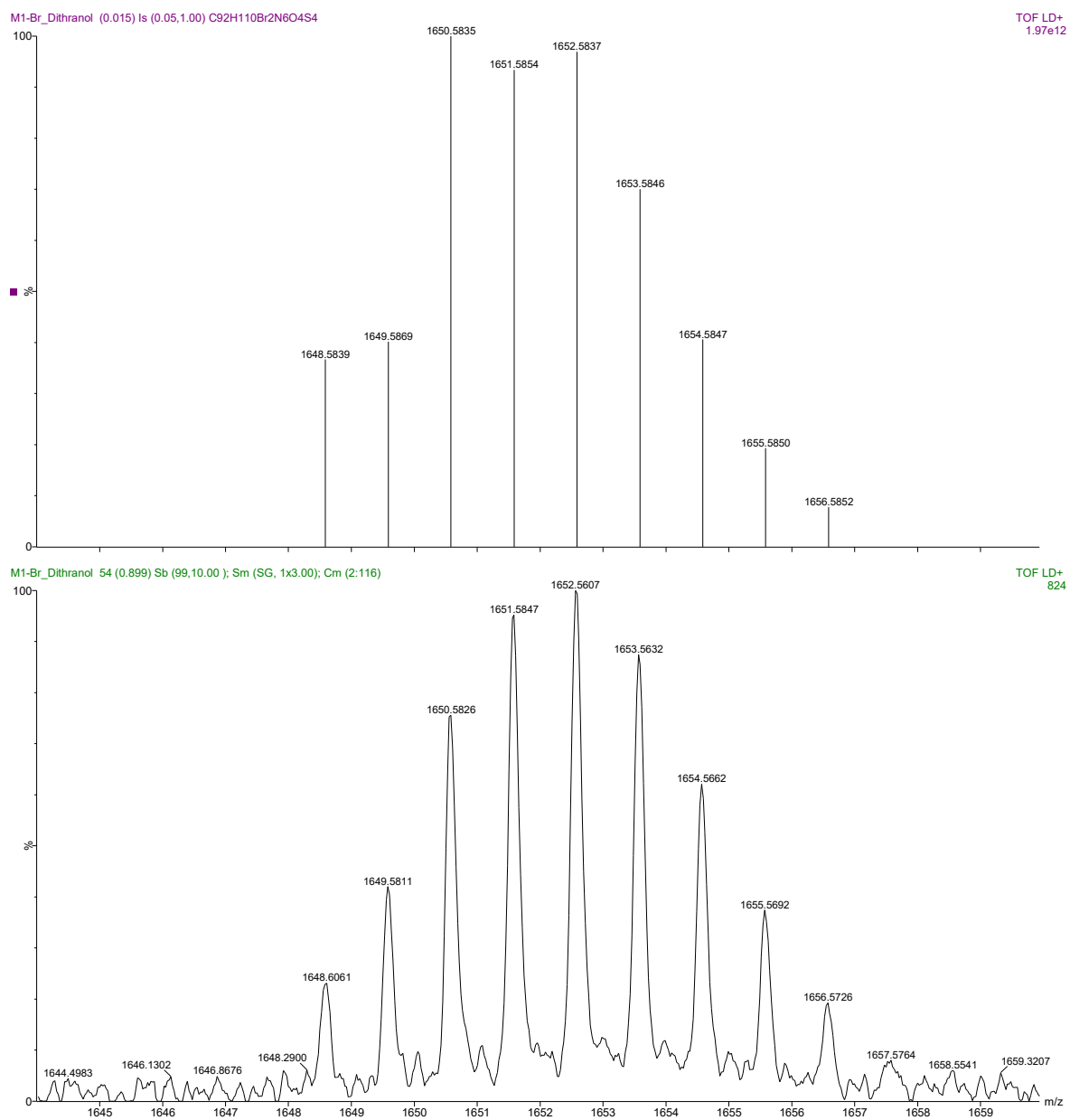
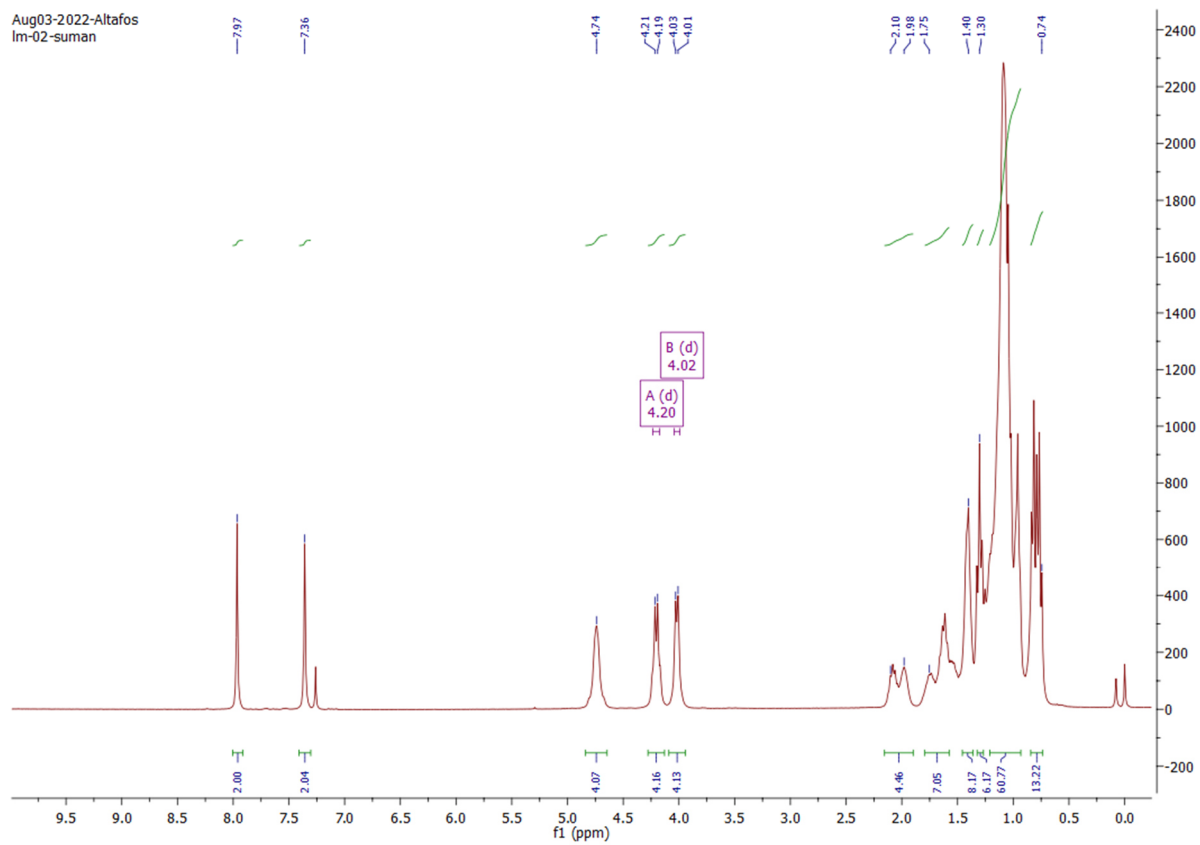**Fig. S10** HR-MS (MALDI-TOF) data of C1 (top: simulated; bottom - measured).

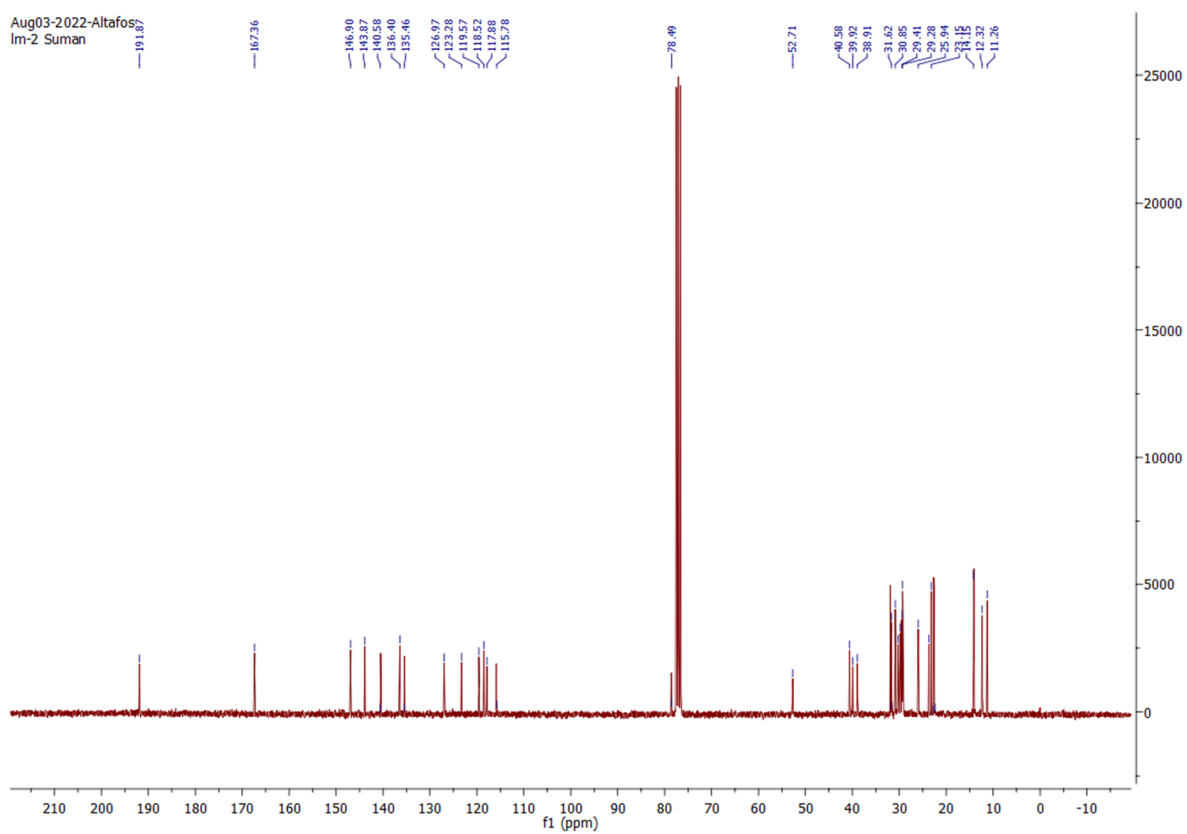**Fig. S11** ^{1}H NMR spectrum of C2 (CDCl$_3$ solution, ppm, 300 MHz).

Fig. S12 ^{13}C NMR spectrum of C2 (CDCl$_3$ solution, ppm, 76 MHz).

100
1426.6598
1427.6403
1428.5967
1429.7003
1430.5590
1431.6144
1415.6539
1416.7281
1417.2411
1419.6355
1424.0145
1425.9003
1434.4879
1436.7496
1437.6842
1440.3175
1442.5592
1443.5449
1444.5313
1447.1216
%
0

M2-S_DCTB (0.017) Is (0.05,1.00) C78H114N4O4S8

TOF LD+
2.69e12

100
1426.6605
1427.6636
1428.6622
%
1429.6626
1430.6617
1431.6614
1432.6606
0

1416 1418 1420 1422 1424 1426 1428 1430 1432 1434 1436 1438 1440 1442 1444 1446 1448 m/z
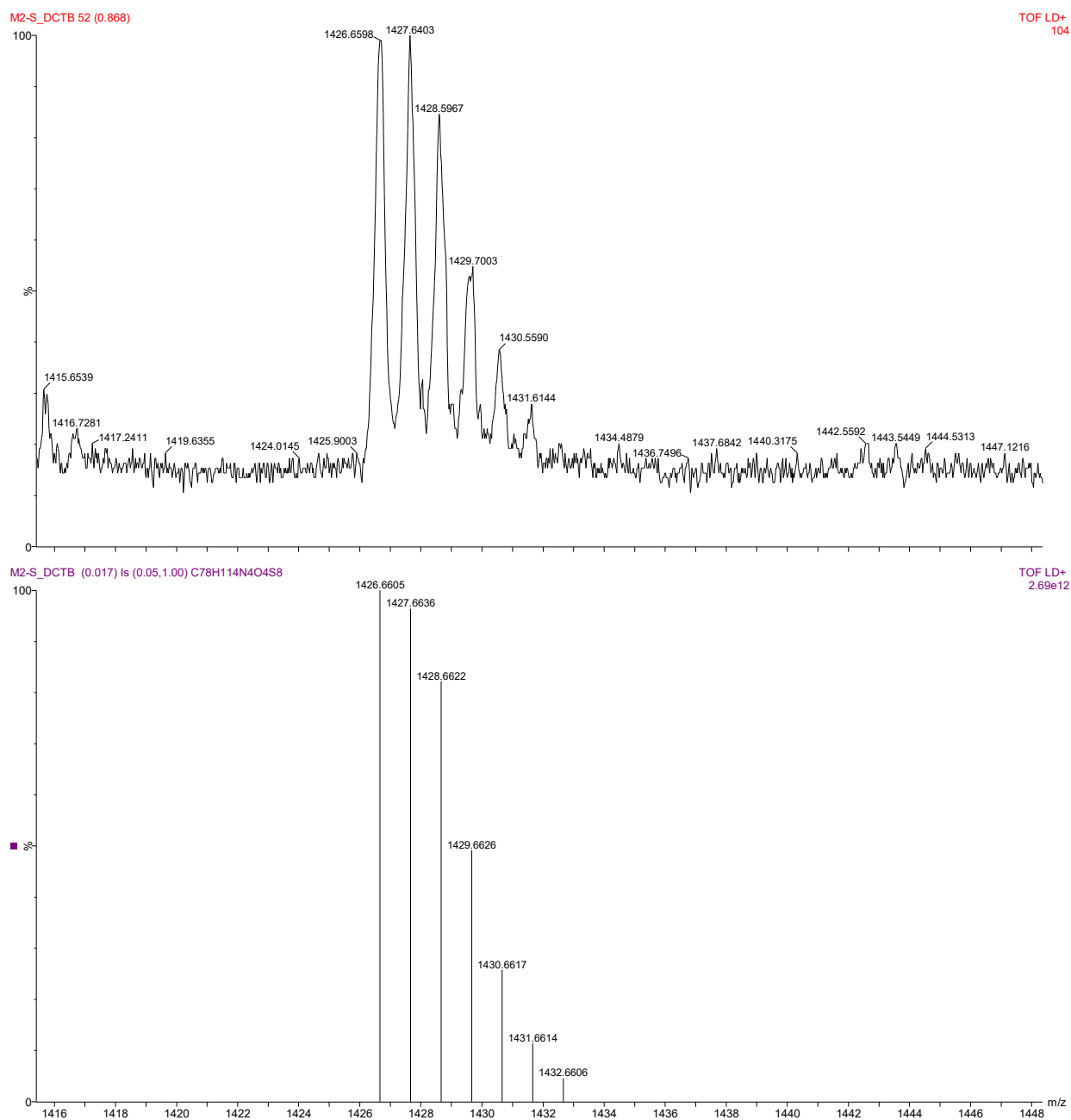
Fig. S13 HR-MS (MALDI-TOF) data of C2 (top: measured; bottom: simulated).

References

(1) C. M. Cardona, W. Li, A. E. Kaifer, D. Stockdale and G. C. Bazan, Electrochemical Considerations for Determining Absolute Frontier Orbital Energy Levels of Conjugated Polymers for Solar Cell Applications, *Adv. Mater.* **2011**, 23, 2367–2371.

(2) J. A. Röhr, D. Moia, S. A. Haque, T. Kirchartz and J. Nelson, Exploring the Validity and Limitations of the Mott–Gurney Law for Charge-Carrier Mobility Determination of Semiconducting Thin-Films, *J. Phys.: Condens. Matter* **2018**, 30, 105901.